Modern Physics Letters B
Vol. 35, No. 21 (2021) 2150359 (16 pages)
© World Scientific Publishing Company
DOI: 10.1142/S0217984921503590

World Scientific
www.worldscientific.com

Mod. Phys. Lett. B 2021.35. Downloaded from www.worldscientific.com
by CHINESE ACADEMY OF SCIENCES on 06/01/22. Re-use and distribution is strictly not permitted, except for Open Access articles.

Electronic property of intrinsic point defect system on β–Si_3N_4 (0001) surface

Lingxia Li, Xuefeng Lu, Jianhua Luo, Xin Guo*, Junqiang Ren,
Hongtao Xue and Fuling Tang

State Key Laboratory of Advanced Processing and Recycling of Non-ferrous Metal,
Department of Materials Science and Engineering,
Lanzhou University of Technology, Lanzhou 730050, China
**guoguox2008@163.com*

Received 5 March 2021
Revised 15 April 2021
Accepted 25 April 2021
Published 4 June 2021

The intrinsic point defect influence data for β–Si_3N_4 by far are incomplete and experimental clarification is not easy. In this contribution, the effects of vacancy (V_{2c}, V_{6h} and V_{Si}) and interstitial (I_N and I_{Si}) defects on the electronic properties of H-passivated β–Si_3N_4 (0001) surface are explored based on density functional theory (DFT) calculation. The results show that it is easier to form N_{6h} vacancy defects in the surface layer under Si-rich conditions. The existence of N vacancies makes the bottom of conduction bands shift downwards, and the top of valance band is away from Fermi level. The presence of V_{Si} makes the system have the characteristics of p-type semiconductor, and the closer to the inner layer, the narrower the range of additional energy bands and the greater the degree of localization of electrons. The closer the Si atom vacancy is to the surface, the smaller the photon energy corresponding to the maximum absorption coefficient is. Compared with the N vacancy system, the Si vacancy system has higher reflection ability in the low energy region. For the interstitial defect systems, I_N is easy to form on the surface layer, and I_{Si} is easy to produce in the inner layer. The I_N system has a new additional energy level at the Fermi level, and as the I_N is closer to the inner layer, the energy range of the additional energy level is also narrower. In the I_{Si} system, the new additional energy levels appear at the Fermi level and the intermediate band. The results have positive significance for the design of this advanced structural and functional integrated ceramics. The absorption coefficient and reflection coefficient of $I_{Si\text{-}3}$ system are much higher than those of other systems when the energy is greater than 2.5 eV.

Keywords: β–Si_3N_4; electrical property; vacancy; interstitial defect.

*Corresponding author.

Mod. Phys. Lett. B 2021.35. Downloaded from www.worldscientific.com
by CHINESE ACADEMY OF SCIENCES on 06/01/22. Re-use and distribution is strictly not permitted, except for Open Access articles.

1. Introduction

Silicon nitride (Si_3N_4) material has been widely used in mechanical processing, metallurgical and chemical industry, aerospace, solar cells and other fields due to its high strength, high temperature resistance and excellent corrosion resistance.[1,2] With the development trend of miniaturization of electronic devices, Si_3N_4 films can also be used as insulating layers, surface passivation, encapsulation and charge trapping materials in microelectronics manufacturing. The bulk electronic structure of Si_3N_4 has been studied extensively by theoretical methods. Grillo *et al.*[3] conducted a comprehensive study of single native point defects in hexagonal silicon nitride (β–Si_3N_4) based on density functional calculations of formation energy. The wide band gap characteristics of Si_3N_4 material can be significantly improved by doping, adsorption, however, under the influence of temperature, radiation, stress and other factors, the atoms in the crystal structure will move and break away from lattice potential field under certain conditions.[4–7] This makes the crystal structure incomplete and limits its use as the basic constituent material of the optoelectronic device. The intrinsic defect exists independently in the crystal structure, and it is found that the existence of N-Vacancy (V_N) defect in α–Si_3N_4 makes the suspended bond of Si produce two defect levels in the band gap of V_N–Si_3N_4, while only one defect level is produced for N substitutional to Si (Si_N) and Si interstitial (Si_I).[8] Similarly, in the α–Si_3N_4 of the absence of nitrogen case, a localized additional energy level is formed in the obvious 4.6 eV wide band gap, allowing electrons to reside in the trap layer of the charge, thus reducing the leakage current, which makes it useful for charge capture storage devices such as charge-trap flash (CTF) memory.[9] Deep level defects are caused by V_N, while the cases are not obvious for H impurities in V_N and Si atoms substituted by V_N, and Si–Si bond or tiny Si clusters formed in Si_3N_4 become the main part of charge capture in memory devices.[10] It has been reported that the surface structure of H-passivated β–Si_3N_4 is more stable and the electron affinity is enhanced. Based on DFT calculations, Bermudez[11] examined the physical and electronic structures of ideal terminated, relaxed and H-saturated β–Si_3N_4 (0001) surfaces. These results will also provide an understanding of the properties of the surface state of β–Si_3N_4 (0001), which has not been discussed in detail before. Tao *et al.*[12] calculated the electron affinities of various clean, hydrogen terminated β–Si_3N_4 surfaces by *ab initio* electronic structure calculation method, and studied various H-covered low index surfaces. It is shown that the prediction of H terminal on β–Si_3N_4 has similar effect on diamond as H terminal: stable H bond and possibility of inducing Also, NEA. Bagatu yants *et al.*[13] studied the chemical reactions on the surface of β–Si_3N_4 (0001) by ab initio (RHF/MP_2) cluster method. Based on these, the electronic structure characteristics of vacancy and interstitial defects on the surface of β–Si_3N_4 (0001) structure with H passivation at both ends were investigated using first principles calculations. By using the formation of a more stable defect system, analyses were conducted on the electronic structure and optical characteristics of each defect

system, which provides theoretical guidance for the practical application of Si_3N_4 materials.

2. Computational Method and Details

The calculations are carried out by the CASTEP code.[14,15] The exchange correlation functional is described by the generalized gradient approximation (GGA) with Perdew–Burke–Ernzerhofer parameterization (PBE).[16,17] At the same time, the ultra-soft pseudopotential method is employed to accurately correct the complex electron–ion interaction during the entire geometric optimization and energy calculation process. The kinetic energy cutoff of plane waves is set to be 400 eV. A Monkhorst pack grid of $4 \times 4 \times 1$ was used. The valence electronic configurations are $3s^2 3p^2$ for Si, $2s^2 2p^3$ for N, $1s^1$ for H, respectively. All the geometric structures are fully relaxed until energy and force are converging to 10^{-5} eV/atom and 0.03 eV/Å, respectively. The vacuum space was set 15 Å to reduce the interactions between neighboring layers in the vertical direction.

The formation energy is one of the parameters to measure the stability of crystal structure with defects, which is given by Ref. 18:

$$E_f = E_{\text{tot}} - n_{\text{Si}}\mu_{\text{Si}} - n_{\text{N}}\mu_{\text{N}} - n_{\text{H}}\mu_{\text{H}} - qE_{\text{F}}, \quad (1)$$

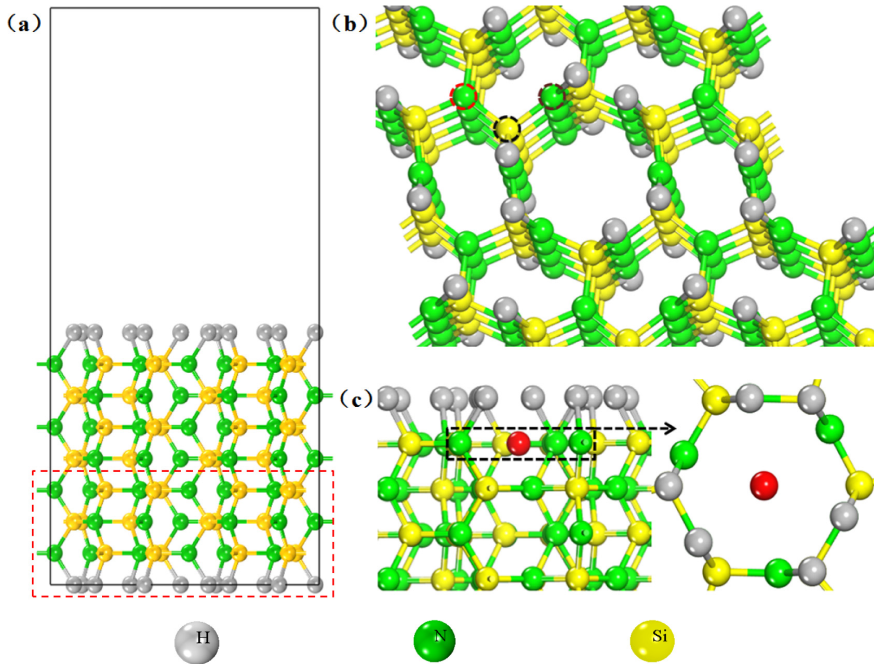

Fig. 1. (Color online) (a) The main view of the supercell model of H passivated β–Si_3N_4 (0001) surface. (b) The red, black and purple dotted circles indicate the positions of $V_{2c\text{-}1}$, $V_{Si\text{-}1}$ and $V_{6h\text{-}1}$, respectively. (c) The main and top views of $I_{N\text{-}1}$ or $I_{Si\text{-}1}$ structure. The red ball represents the interstitial atom.

Mod. Phys. Lett. B 2021.35. Downloaded from www.worldscientific.com
by CHINESE ACADEMY OF SCIENCES on 06/01/22. Re-use and distribution is strictly not permitted, except for Open Access articles.

where E_{tot} is the total energy of the system with intrinsic point defects, n_{Si}, n_{N} and n_{H} represent the number of Si, N and H atoms in the supercell, respectively. μ_{Si}, μ_{N}, μ_{H} are chemical potentials of Si, N and H atoms, respectively. q represents the charged state, and E_{F} represents the Fermi energy. Under N-rich conditions, $\mu_{\text{N}} = \mu_{(\text{N}_2)}/2$, $\mu_{\text{Si}} = (\mu_{(\beta-\text{Si}_3\text{N}_4)} - 4\mu_{\text{N}})/3$, and under Si-rich conditions, $\mu_{\text{Si}} = \mu_{\text{Si}}^{\text{bulk}}$, $\mu_{\text{N}} = (\mu_{(\beta-\text{Si}_3\text{N}_4)} - 3\mu_{\text{Si}})/4$.

In order to better display the distortion of surrounding atoms when defects are formed, a seven-layer structure model of β–Si_3N_4 (0001) surface passivated by hydrogenation on the upper and lower surfaces is adopted. According to the convergence test on the number of released atomic layers, the H atomic layer at the bottom and the three Si–N atomic layers connected with it are fixed, as shown in Fig. 1(a). In Fig. 1(b), N atom vacancy defects at 2c and 6h position in the first layer are represented by symbol of $\text{V}_{\text{2c-1}}$, $\text{V}_{\text{6h-1}}$, respectively, and Si atom vacancy defects in the first layer are represented by symbol of $\text{V}_{\text{Si-1}}$ silicon vacancy (V_{Si}). Nitrogen interstitial (I_{N}) and silicon interstitial (I_{Si}) are shown in Fig. 1(c). In order to be able to clearly distinguish the atomic layer where the point defect is located, it can be expressed as $\text{V}_{\text{2c-n}}$ ($\text{V}_{\text{6h-n}}$), $\text{V}_{\text{Si-n}}$ and $\text{I}_{\text{N-n}}$ ($\text{I}_{\text{Si-n}}$), in which n represents the number of atomic layers, which are integers 1, 2 and 3, respectively.

3. Results and Discussion

3.1. *Crystal structure of vacancy systems*

Figures 2(a)–2(c) show the optimized local diagram of three vacancy systems ($\text{V}_{\text{2c-1}}$, $\text{V}_{\text{6h-1}}$, $\text{V}_{\text{Si-1}}$). Due to the lack of atoms, the bond lengths of the atoms around the missing atoms are changed after optimization. For the $\text{V}_{\text{2c-1}}$ system, the surrounding Si atoms move inward, the distance between adjacent Si atoms is reduced by about 7.9%, and the bond length between the surrounding Si atoms and its neighboring N and H atoms are significantly shorter (bond lengths of Si–N and Si-H are 1.709 Å, 1.490 Å). After the optimization of the $\text{V}_{\text{6h-1}}$ system, it can be clearly seen that the H atom connected to the N atom tends to the position of the original N atom and forms a bond with the adjacent Si atom, simultaneously, Si atom remove outward. After the optimization of $\text{V}_{\text{Si-1}}$ system, the H atom connected with the original Si atom moves to the adjacent N_{6h} atom in the first layer, and the bond length of N-H after bonding is 1.307 Å.

In the second and third layer vacancy systems, the distance between adjacent Si atoms is significantly larger than that between Si atoms in the first layer, which is close to the case of N_{2c} atom missing in bulk phase. In $\text{V}_{\text{6h-2}}$ and $\text{V}_{\text{6h-3}}$ systems, the structural distortion of adjacent atoms becomes smaller after optimization, and the situation is similar for $\text{V}_{\text{Si-2}}$ and $\text{V}_{\text{Si-3}}$ systems. This shows that the surface vacancy defects have a greater impact on the structure, while the inner layer vacancy defects have a relatively small impact on the structure.

Table 1 shows the formation energies (E_f) of all β-Si_3N_4 (0001) supercells with intrinsic point defects under various vacancy conditions in the neutral charge state

Mod. Phys. Lett. B 2021.35. Downloaded from www.worldscientific.com
by CHINESE ACADEMY OF SCIENCES on 06/01/22. Re-use and distribution is strictly not permitted, except for Open Access articles.

Mod. Phys. Lett. B 2021.35. Downloaded from www.worldscientific.com
by CHINESE ACADEMY OF SCIENCES on 06/01/22. Re-use and distribution is strictly not permitted, except for Open Access articles.

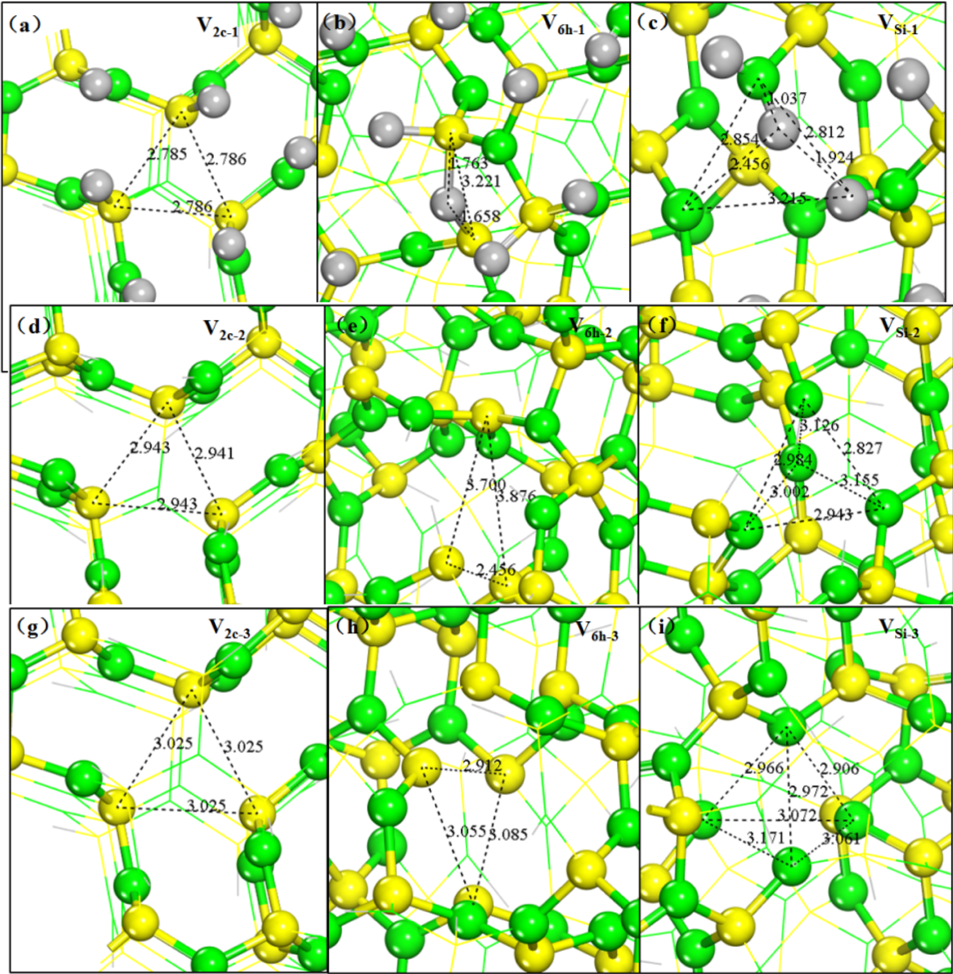

Fig. 2. (Color online) The structure diagram of vacancy atoms on β–Si$_3$N$_4$ (0001) surface passivated by H. Vacancy structure of (a)–(c) the first layer, (d)–(f) the second layer and (g)–(i) the third layer.

Table 1. Formation energies of vacancy systems.

	$V_{2c\text{-}1}$	$V_{6h\text{-}1}$	$V_{Si\text{-}1}$	$V_{2c\text{-}2}$	$V_{6h\text{-}2}$	$V_{Si\text{-}2}$	$V_{2c\text{-}3}$	$V_{6h\text{-}3}$	$V_{Si\text{-}3}$
E_f/eV (Si-rich)	2.881	1.711	5.107	3.303	2.761	11.101	3.078	3.456	11.101
E_f/eV (N-rich)	3.213	2.043	4.662	3.635	3.092	10.646	3.410	3.788	10.566

($q = 0$). It can be distinctly observed that E_f is sensitive to environment, and the values are positive under the conditions that N-rich and Si-rich. The lower the formation energy, the more stable the system is, from a view of thermodynamic. The formation energy of N vacancy system under Si-rich conditions is lower than that of

N vacancy system under N-rich conditions, which is consistent with the formation energy of bulk N vacancies.[19] In contrast, the formation energies of Si vacancies are all higher than those of different vacancy systems under N-rich conditions, indicating that N atom vacancy defects are easily formed under Si-rich conditions. Meanwhile, the formation energies of vacancy systems in the first layer are less than those of the second and third vacancy systems, regardless of the Si-rich or N-rich conditions, indicating that vacancies are more likely to appear near the surface. The shorter the distance of the vacancy is from the surface, the lower formation energy, indicating that the closer the vacancy is to the surface, the more likely it is to appear. In addition, $V_{6h\text{-}1}$ system has the lowest formation energy in Si-rich environment. Therefore, it can be concluded that N atomic vacancies are easily formed under this condition, while the surface H atoms tend to move to the position of the original N atoms and bond with adjacent Si atoms to obtain a new stable structure.

3.2. *Electronic properties of vacancy systems*

Figure 3 shows the band structures and partial density states (PDOS) of the perfect and vacancy systems. The red dotted line represents the Fermi level. As shown in Fig. 3(a), it can be seen from the band structure of H passivated β–Si_3N_4 (0001) surface that the band gap is 4.20 eV. The effect of dangling bonds is not eliminated due to passivation of H atom on the upper and lower surfaces, and the intermediate bands are generated. Combined with the partial density of states, it is known that this is mainly the *s* orbital contribution of H atoms, which is in accordance with the previous report.[20] Besides, the intermediate bands of 1.47 ∼ 1.71 eV and 0.92 ∼ 1.07 eV are also caused by the Si and N atoms connected to H atoms in the bottom fixed layer. It is interesting that in the range of 3.71–3.99 eV, the band at the bottom of the conduction band is mainly due to the action of H atoms and adjacent Si and N atoms in the first layer.

The results show that the band gap of the system decreases obviously when N atom vacancies appear in the first Si–N atomic layer, but increases when Si atom vacancies are formed. The conduction band and intermediate band are close to the Fermi level in three cases. Among this, the valence band of the N vacancy system is far away from the Fermi level, while a new additional energy level at the Fermi level is present in the Si vacancy system, which is mainly attributed to the unsaturated bonds of N atoms around the vacancy of Si atoms, leading to the characteristic of *p*-type semiconductor. Compared with the perfect system, the number of the intermediate bands near the bottom of the conduction band increases owing to the absence of N atoms, and this is mainly caused by the contribution of *p*-orbital electrons of Si, as shown in Figs. 3(c) and 3(d). Obviously, in $V_{2c\text{-}1}$ system, the intermediate band near the bottom of conduction band becomes wider, which weakens the electron localization. The state density range formed by *p*-orbital electrons of Si is 1.82–2.22 eV, larger than those of other systems.

Mod. Phys. Lett. B 2021.35. Downloaded from www.worldscientific.com
by CHINESE ACADEMY OF SCIENCES on 06/01/22. Re-use and distribution is strictly not permitted, except for Open Access articles.

Mod. Phys. Lett. B 2021.35. Downloaded from www.worldscientific.com
by CHINESE ACADEMY OF SCIENCES on 06/01/22. Re-use and distribution is strictly not permitted, except for Open Access articles.

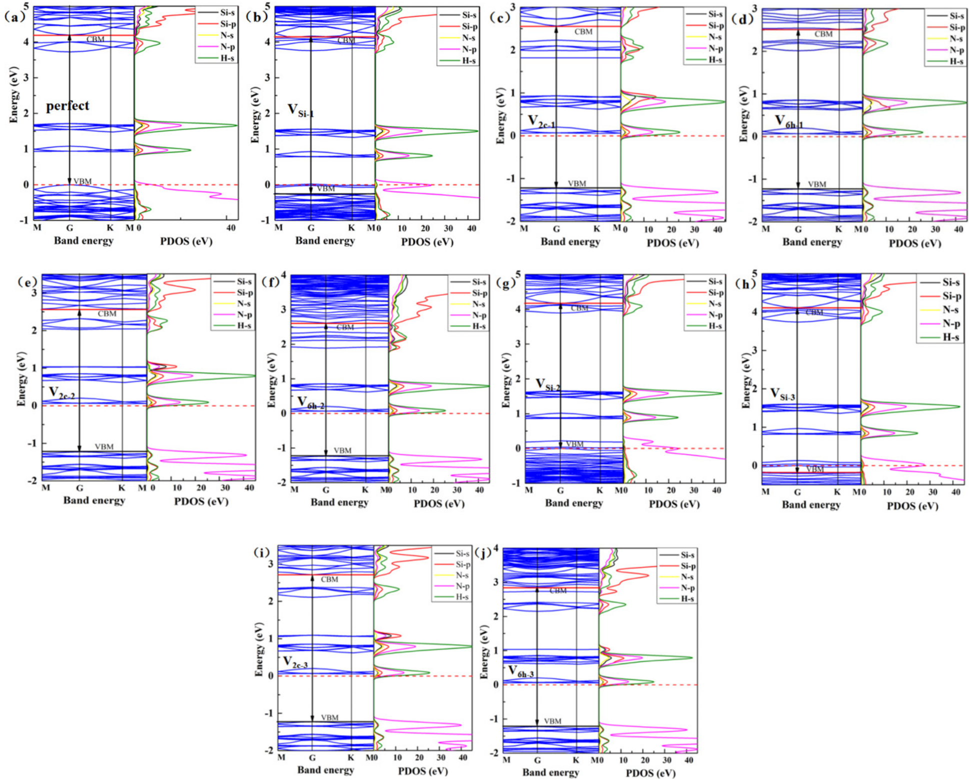

Fig. 3. (Color online) The band structures and partial density of states for perfect (a), vacancy (b)–(j) systems.

When the single atom vacancy appears in the inner layer (the second and third Si–N layers), the band gap of N-deficient system decreases in varying degrees, while that of Si vacancy system increases, which is similar to that of the first layer. In the Si vacancy system, the three additional energy levels near the Fermi level become more concentrated, which indicates that the degree of electron localization is enhanced. In the corresponding partial density of states, it can be observed that sharp peaks occur at the Fermi level, attributed to the contribution of N-p orbitals, as shown in Figs. 3(g) and 3(h). For the N atom vacancy system, the number of intermediate bands around 1 eV increases mainly due to the contribution of the p-orbital of the surrounding Si atoms. At the same time, closer to the inner layer, the position of the additional energy level gradually stabilizes at 1 eV. This energy level belongs to a deep level, which will cause the recombination of holes and electrons to reduce the concentration of carriers.

3.3. *Optical properties of vacancy systems*

Figures 4(a)–4(j) are the absorption coefficient of the perfect system and the vacant system. It can be seen that the absorption coefficients of all vacancy systems

Mod. Phys. Lett. B 2021.35. Downloaded from www.worldscientific.com
by CHINESE ACADEMY OF SCIENCES on 06/01/22. Re-use and distribution is strictly not permitted, except for Open Access articles.

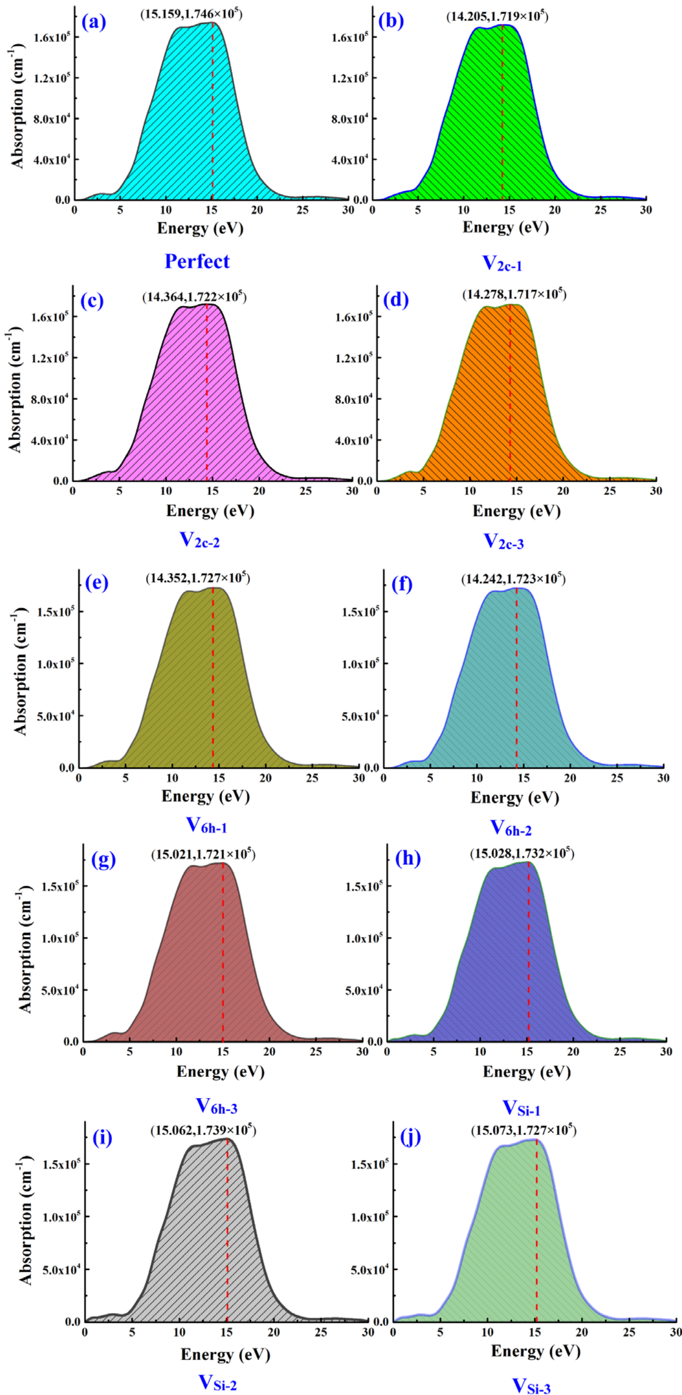

Fig. 4. (Color online) Absorption spectra of perfect system and vacant system.

Mod. Phys. Lett. B 2021.35. Downloaded from www.worldscientific.com
by CHINESE ACADEMY OF SCIENCES on 06/01/22. Re-use and distribution is strictly not permitted, except for Open Access articles.

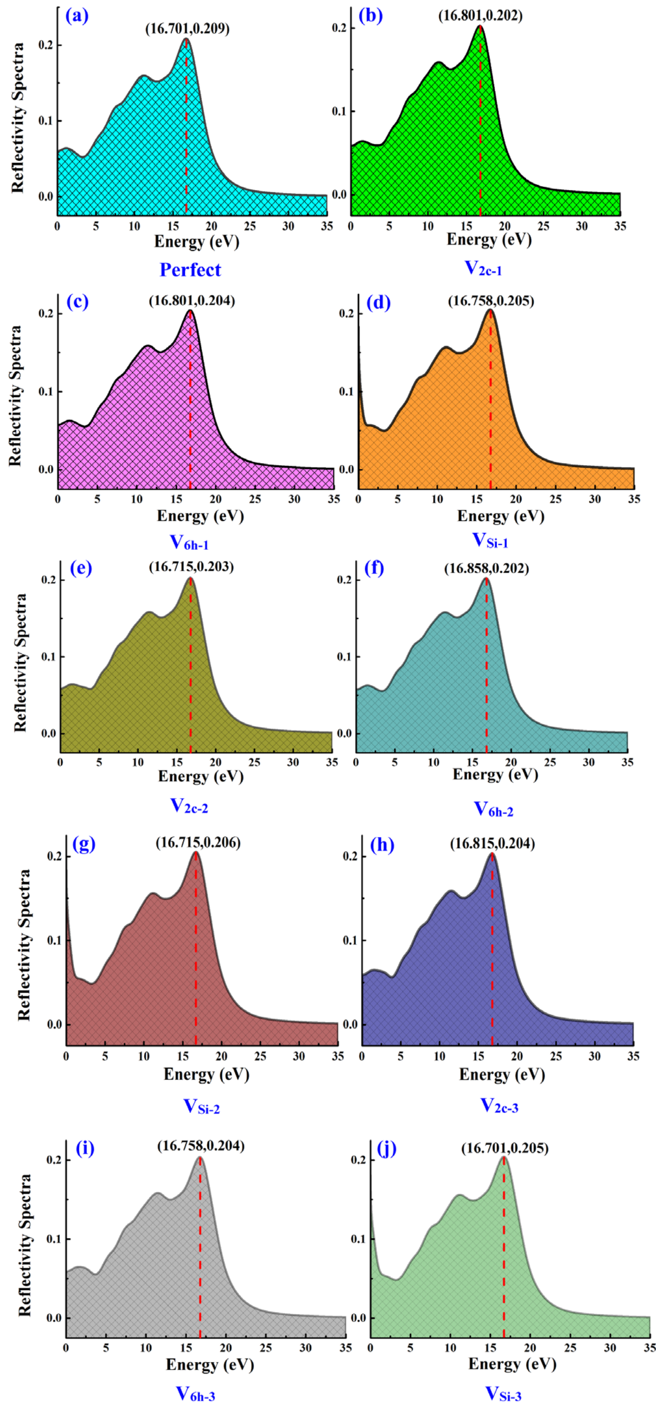

Fig. 5. (Color online) Reflectance spectrum of perfect system and vacant system.

show a similar trend with the increase of photon energy. In the range of $0 \sim 5$ eV photon energy, the absorption coefficient curve first increases and then slightly decreases, and then the first peak appears at about 10 eV, and the maximum absorption coefficient is reached near 15 eV, and then as the photon energy increases, the absorption coefficient drastically reduced. For the perfect system, the highest absorption peak appears at 15.159 eV. Compared with bulk β–Si_3N_4, the photon energy is larger. When there are vacancies in the structure, the photon energy corresponding to the highest absorption peak is less than the perfect system, and the absorption peak is also lower than the perfect system. It is found that in the same Si–N atomic layer, that is, $V_{2c\text{-}1}$, $V_{6h\text{-}1}$ and $V_{Si\text{-}1}$ systems, the corresponding maximum absorption peaks are $(14.205, 1.719 \times 10^5)$, $(14.353, 1.727 \times 10^5)$ and $(15.028, 1.732 \times 10^5)$, respectively. The photon energy $V_{2c\text{-}1} < V_{6h\text{-}1} < V_{Si\text{-}1}$, the highest peak also shows $V_{2c\text{-}1} < V_{6h\text{-}1} < V_{Si\text{-}1}$. In different Si–N atomic layers, the closer the Si atom vacancy is to the surface layer, the smaller the photon energy corresponding to the maximum absorption coefficient. In addition, for both perfect and vacant systems, the maximum absorption coefficient appears in the ultraviolet region ($3.5 \sim 15.5$ eV), while the absorption capacity in the visible light region ($1.5 \sim 3.5$ eV) is weak. This can provide a theoretical basis for the application of this material in the field of photosensitive devices in the ultraviolet region.

The reflection spectra of the perfect system and the vacant system are shown in Fig. 5. It can be seen that when there are Si atom vacancies in different Si–N atomic layers, the local minimum is reached at about 4 eV, the first reflection peak appears at about 11 eV, and the strongest reflection peak appears near 16 eV. The change trend of the reflection spectrum of the N vacancy system in different Si–N atomic layers is similar to that of the perfect system. The reflectance spectrum of the perfect system reaches the maximum value of 0.209 at 16.701 eV, and the reflectance approaches zero when the photon energy exceeds 25 eV. In addition, compared with the perfect system, the corresponding photon energy of each vacancy defect system has increased, that is, the phenomenon of blueshift occurs when single vacancies appear in different Si–N atomic layers. In the visible light energy range, the reflectivity has a downward trend. From the results of both absorption coefficient and reflectivity, it is found that Si vacancies in the Si–N atomic layer have a greater impact than N vacancies, which can provide a theoretical basis for applications in the field of photosensitive detection.

3.4. *Crystal structure of interstitial systems*

Since the atomic arrangement on the surface of β–Si_3N_4 (0001) is the same as one end of the bulk phase, a $2 \times 2 \times 7$ supercell structure model is constructed. The Si or N atoms are placed at the center of the ring, and the Z-direction coordinate of the interstitial atoms is set to be consistent with that of the atoms in the same layer. The geometrically optimized structure of the three-layer interstitial defect system is shown in Figs. 6(a)–6(f). Since the radius of the interstitial Si atom is

Mod. Phys. Lett. B 2021.35. Downloaded from www.worldscientific.com
by CHINESE ACADEMY OF SCIENCES on 06/01/22. Re-use and distribution is strictly not permitted, except for Open Access articles.

Mod. Phys. Lett. B 2021.35. Downloaded from www.worldscientific.com
by CHINESE ACADEMY OF SCIENCES on 06/01/22. Re-use and distribution is strictly not permitted, except for Open Access articles.

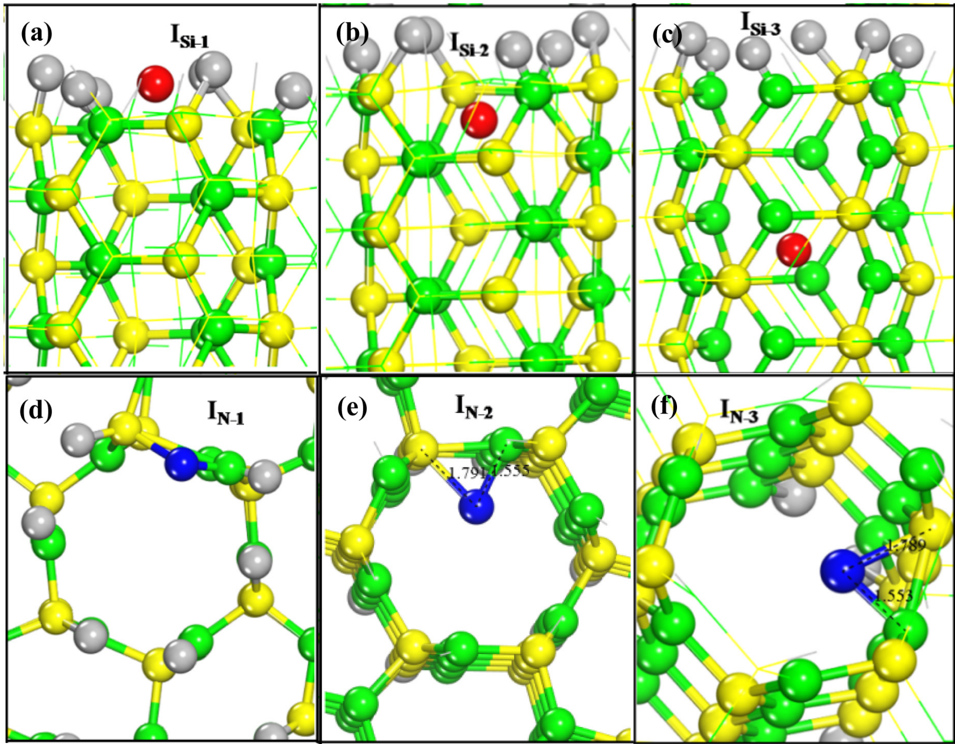

Fig. 6. (Color online) The structure diagram of interstitial atoms on β–Si_3N_4 (0001) surface passivated by H. Interstitial structure of (a)–(c) Si N atoms and (d)–(f) N atoms in different layers.

larger than that of the N atom (1.123 Å for Si atom and 0.699 Å for N atom),[21] the Si atoms initially located at the center of the hexagon only diffuse to the interlayer along the Z direction after the optimization of $I_{\text{Si-1}}$, $I_{\text{Si-2}}$, $I_{\text{Si-3}}$ systems, but the diffusion direction of Si atoms in the first and second layers is different from that of Si atoms in the third layer. This result is also shown by the fractional coordinates after diffusion of the Si atoms filled in different layers, as listed in Table 2. For the N interstitial system, $I_{N\text{-}1}$, $I_{\text{N-2}}$ and $I_{\text{N-3}}$ systems are similar after optimization, the diffusion of interstitial atoms mainly occurs in the atomic layer plane with the variable quantity range of 0.91–9.42% in the Z direction, and news Si–N bonds and N–N bonds are formed on the six-membered ring. The bond length of the new Si–N bond formed is longer than that of the N–N bond.

Table 3 shows the formation energies of six kinds of interstitial defect systems. Comparing $I_{\text{N-1}}$ and $I_{\text{Si-1}}$ systems, the formation energy of interstitial N atoms is lower than that of Si interstitials, which indicates that interstitial defects of N atoms are more likely to appear on the surface. When Si or N atoms fill in the inner layer, the formation energy is higher than that of the outer layer, so it is difficult to form the interstitial defects inner layer. Compared with $I_{\text{N-2}}$, $I_{\text{Si-2}}$, $I_{\text{N-3}}$ and $I_{\text{Si-3}}$ systems,

Table 2. Fractional coordinates of interstitial atoms after geometric optimization.

Interstitial atoms	Initial fractional coordinates	Fractional coordinates optimized
N-1	(0.5, 0.5, 0.382)	(0.379, 0.351, 0.418)
Si-1		(0.5, 0.5, 0.417)
N-2	(0.5, 0.5, 0.327)	(0.433, 0.487, 0.330)
Si-1		(0.5, 0.5, 0.358)
N-3	(0.5, 0.5, 0.273)	(0.569, 0.513, 0.276)
Si-3		(0.5, 0.5, 0.244)

Table 3. Formation energies of interstitial defect systems.

	$I_{N\text{-}1}$	$I_{Si\text{-}1}$	$I_{N\text{-}2}$	$I_{Si\text{-}2}$	$I_{N\text{-}3}$	$I_{Si\text{-}3}$
E_f (eV) (Si-rich)	4.904	5.173	6.894	5.663	6.987	5.581
E_f (eV) (N-rich)	4.574	5.627	6.562	6.109	6.655	6.027

the formation energy of N atom interstitial is significantly higher than that of Si atom interstitial, which is opposite to that on the outer surface. Combined with Table 1, it is found that the formation energy of N vacancy system in the same layer is lower than that of N-interstitial system. The case is also observed for Si vacancy system and Si interstitial system in the surface layer, nevertheless, it is noteworthy that Si vacancy in the inner layer is more difficult to form than the Si interstitial system. From the above, it can be concluded that N atom vacancy defects are easy to form on the surface layer, while Si atom interstitial defects are more likely to emerge in the inner layer. This can provide reference for the preparation and application of this thin layer material.

3.5. *Electronic properties of interstitial systems*

Figures 7(a)–7(c) display the band structures of the defect system when N atoms are interspersed in different Si–N atomic layers. Since the existence of interstitial N atoms, the energy range corresponding to the energy band has changed significantly. The energy bands above Fermi level move to Fermi level, while the valence bands are far away from Fermi level as a whole. There is almost no change in the energy range of the three groups of intermediate bands, indicating that the effective mass of electrons is small and the localization degree is weak. The band gap values of $I_{N\text{-}1}$, $I_{N\text{-}2}$ and $I_{N\text{-}3}$ system are 4.30 eV, 4.22 eV and 4.21 eV, respectively, which are all increased compared with the perfect system. Interestingly, new additional energy levels located at the Fermi level appear in the system owing to the presence of interstitial N atoms. The two new additional energy levels in the $I_{N\text{-}2}$ and $I_{N\text{-}3}$ systems are located at the Fermi level and the top of the valence band, respectively, and the energy value corresponding to the additional energy level at the top of the valence band varies with the position of the interstitial N atom. This energy level is classified as a deep impurity level, which can affect the recombination of carriers

Mod. Phys. Lett. B 2021.35. Downloaded from www.worldscientific.com
by CHINESE ACADEMY OF SCIENCES on 06/01/22. Re-use and distribution is strictly not permitted, except for Open Access articles.

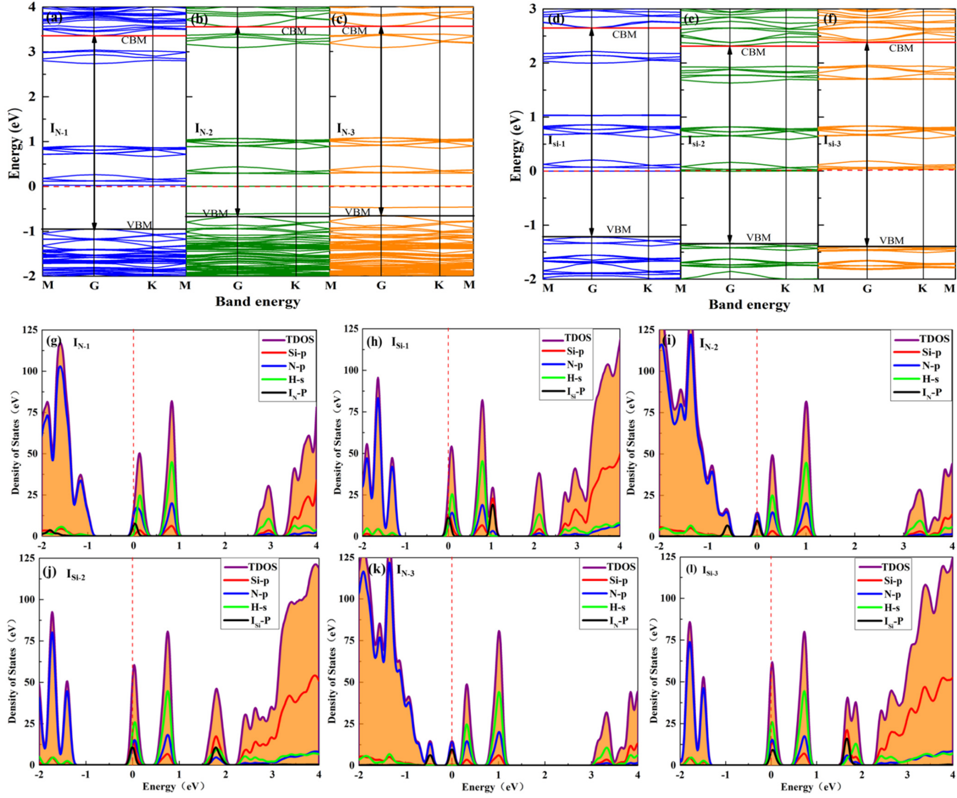

Fig. 7. (Color online) The band structures (a)–(f) and Partial density of states (g)–(l) of interstitial systems.

and reduce their lifetime. The band structures of Si interstitial systems are shown in Figs. 7(d)–7(f). The energy position is the same as that of N atom interstitial in virtue of the interstitial Si atom, and the valence bands are far away from Fermi level totally. The band gap values of the $I_{\text{Si-1}}$, $I_{\text{Si-2}}$ and $I_{\text{Si-3}}$ systems are 3.86 eV, 3.64 eV and 3.76 eV, respectively, which are smaller than that of perfect system. There is an obvious additional energy level at 1.03 eV in the $I_{\text{Si-1}}$ system, which also belongs to the deep energy level.

Figures 7(g)–7(l) show the total and partial density of states of each interstitial system. For the existence of interstitial atoms, impurity states appear at the Fermi level, which is mainly attributed to the contribution of *p* orbitals of interstitial atoms. For the N-interstitial systems, there are new electronic states below the Fermi level. It is thus clear that the new additional energy levels in the $I_{\text{N-2}}$ and $I_{\text{N-3}}$ systems are caused by the contribution of the *p* orbitals of the interstitial N atom. The closer the interstitial atom is to the inner layer, the closer the new impurity state is to the Fermi level. For the Si-interstitial systems, new electronic states appear in the Fermi level. The closer the interstitial atom is to the inner layer,

Mod. Phys. Lett. B 2021.35. Downloaded from www.worldscientific.com by CHINESE ACADEMY OF SCIENCES on 06/01/22. Re-use and distribution is strictly not permitted, except for Open Access articles.

the farther the new impurity state is to the Fermi level. When the interstitial Si atom is in the second and third layers, the new impurity state gradually stabilizes at the energy position of the surface state caused by the release of the surface atomic layer. Furthermore, it increases the localization of the intermediate band electrons and increases the electron density.

3.6. *Optical properties of interstitial systems*

The absorption spectrum of the perfect system and the interstitial system of N and Si atoms is shown in Fig. 8(a). It can be clearly seen that as the photon energy increases, the highest absorption coefficient of all interstitial systems is concentrated around 16 eV. When the energy is greater than 5 eV, the change trend of the absorption coefficient of each system is almost the same except for the $I_{Si\text{-}3}$ system. For $I_{Si\text{-}3}$ system, a high absorption peak appears at 0.0983 eV, which indicates that the absorption capacity of Si atom is enhanced in the low energy range, which is slightly higher than that of perfect system and other interstitial systems in the energy range of $4 \sim 6$ eV, and the absorption coefficient is very low when it exceeds 24 eV, which indicates that the absorption of light system is not sensitive enough in this wave band. The variation of reflectance curves of individual system is shown in Fig. 8(b). The Si atom interstitial system in the inner layer, especially in the third layer, has obvious changes compared with other systems. It has high reflectivity in the low energy range, and its value can reach about 0.7. With the increase of energy in the energy range of $2.26 \sim 9.14$ eV, it is lower than the perfect system and other interstitial systems, and the highest reflectivity is 0.219 when the photon energy is 16.889 eV, which shows a blueshift phenomenon compared with the perfect system. Considering both absorption coefficient and reflectivity, the interstitial Si atoms in the inner layer have a greater influence on the absorption and reflection of light waves than the interstitial atoms on the surface. This is an important guide for the application of Si_3N_4 thin film materials as anti-reflection coating materials.

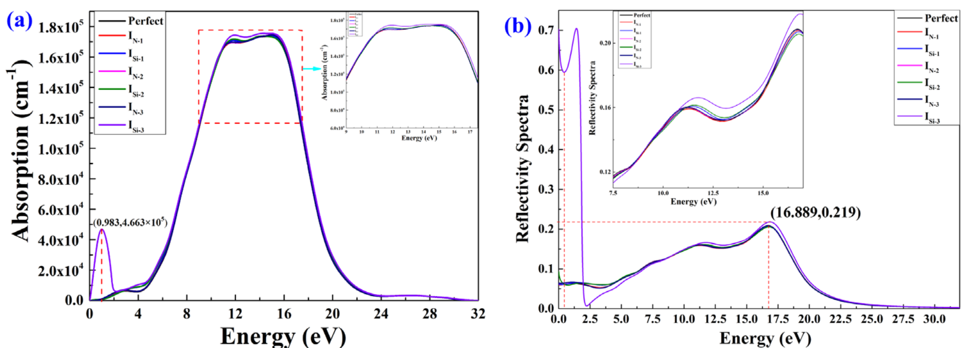

Fig. 8. (Color online) Absorption spectrum and reflection spectrum of perfect (a) and interstitial defect system (b).

Mod. Phys. Lett. B 2021.35. Downloaded from www.worldscientific.com
by CHINESE ACADEMY OF SCIENCES on 06/01/22. Re-use and distribution is strictly not permitted, except for Open Access articles.

Mod. Phys. Lett. B 2021.35. Downloaded from www.worldscientific.com
by CHINESE ACADEMY OF SCIENCES on 06/01/22. Re-use and distribution is strictly not permitted, except for Open Access articles.

4. Conclusion

The structural, electronic and optical properties of the single-atom vacancies and interstitial defects on the surface of β–Si_3N_4 (0001) are performed on account of the first principles calculations. For the single-atom vacancy defect systems of different layers, it shows that the $V_{6h\text{-}1}$ system is easier to form under Si-rich conditions, and the formation energy is higher when the Si vacancy is closer to the inner layer. The existence of N vacancy makes the bottom of conduction band move down, the top of valence band is far away from Fermi level, and a new additional energy level is produced in the middle bands. The existence of Si vacancy makes new energy levels appear at the top of valence band and Fermi level. The closer to the inner layer, the narrower the energy range of the additional energy band, the greater the degree of electron localization and the sharper the peak value of the density of states. The closer the Si atom vacancy is to the surface, the smaller the photon energy corresponding to the maximum absorption coefficient is. Compared with the N vacancy system, the Si vacancy system has higher reflection ability in the low energy region. For the monoatomic interstitial defect system of different layers, N atom interstitial defect is easy to form in the surface layer, while Si atom interstitial defect is easy to appear in the inner layer, compared with the vacancy system, N atom interstitial defect is more difficult to form. New additional energy levels appear at Fermi level in N-interstitial system, while new energy levels appear in Si interstitial system at Fermi level and intermediate band near the bottom of conduction bands. The absorption coefficient and reflection coefficient of $I_{Si\text{-}3}$ system are much higher than those of other systems when the energy is greater than 2.5 eV.

Acknowledgments

The work was supported by the National Natural Science Foundation of China (Grant Nos. 51662026 and 52061025), Joint fund between Shenyang National Laboratory for Materials Science and State Key Laboratory of Advanced Processing and Recycling of Nonferrous Metals (Grant No. 18LHPY001).

References

1. X.-Y. Zhang, W. L. Huo, F. Qi, Y. N. Qu, J. Xu, K. Gan, N. Ma and J. L. Yang, *J. Am. Ceram. Soc.* **99** (2016) 2920.
2. X. Lu, J. Luo, P. Yang *et al.*, *Mod. Phys. Lett. B* **36** (2019) 1950451.
3. M. E. Grillo, S. D. Elliott and C. Freysoldt, *Phys. Rev. B* (2011) 83085208.
4. Y. C. Ding, A. P. Xiang, M. Xu and W. J. Zhu *Physica B* **403** (2008) 2200.
5. X. Tong, J. Li, X. Yang, H. Lin, G. Guo and M. He, *J. Am. Ceram. Soc.* **89** (2006) 1730.
6. Q. Yang, Z. Chen, X. Yang, D. Zhou, X. Qian, J. Zhang and D. Zhang, *Mater. Lett.* **212** (2018) 41.
7. S.-H. Fang, X.-L. Cheng, Y. Huang and H.-H. Gu, *Acta Phys. Sin.* (2007) 6634.

8. Z. Huang, F. Chen, R. Su, Z. Wang, J. Li, Q. Shen and L. Zhang, *RSC Adv.* (2016) 67568.
9. G. Kang, D. Lee, K. Lee, J. Kim and S. Han, *Phys. Rev. Appl.* **10** (2018) 064052.
10. C. Di Valentin, G. Palma and G. Pacchion, *J. Phys. Chem. C* **115** (2011) 561.
11. V. M. Bermudez, *Surf. Sci.* **579** (2005) 11–20.
12. S. X. Tao, A. Theulings and J. Smedley, *Diamond Related Mater.* **53** (2015) 52–57.
13. A. A. Bagatur'yants, K. P. Novoselov, A. A. Safonov, J. V. Cole, M. Stoker and A. A. Korkin, *Surf. Sci.* **486** (2001) 213.
14. Z. Huang, F. Chen, R. Su, Z. Wang, J. Li, Q. Shen and L. Zhang, *J. Alloys Compd.* **637** (2015) 376.
15. X. Lu, X. Gao, J. Ren, C. Li, X. Guo, X. Yan and P. La, *Comp. Mater. Sci.* **151** (2018) 296.
16. P. Yang, F. Xu, J. Li, H. Wu, G. Nie, Y. Shao and S. Wu, *J. Eur. Ceram. Soc.* **40** (2020) 5293.
17. N. Chen, Y. Chen, J. Ai, C. Li, P. He, J. Ren and Q. Zhu, *Appl. Surf. Sci.* **434** (2018) 211.
18. K. Tatsumi, I. Tanaka and H. Adachi, *J. Am. Ceram. Soc.* **85** (2002) 97.
19. G. Hartmann, P. L. G. Ventzek, T. Iwao, K. Ishibashic and S. Gyeong Hwang, *Phys. Chem. Chem. Phys.* **20** (2018) 29152.
20. V. M. Bermudez, *Surf. Sci.* **691** (2020) 121511.
21. C. H. Suresh and N. Koga, *J. Phys. Chem. A* **105** (2001) 5940.

Mod. Phys. Lett. B 2021.35. Downloaded from www.worldscientific.com
by CHINESE ACADEMY OF SCIENCES on 06/01/22. Re-use and distribution is strictly not permitted, except for Open Access articles.